August 24, 1999

Torque Bias Profile for Improved Tracking of the Deep Space Network Antennas

W. Gawronski[1], J.J. Brandt[2], H.G. Ahlstrom, Jr.[1], and E. Maneri[3]

[1] Communications Ground Systems Section
Jet Propulsion Laboratory
California Institute of Technology
Pasadena, CA 91109
Tel.: (818) 354-1783
E-mail: wodek.k.gawronski@jpl.nasa.gov

[2] University of Washington, Seattle, WA

[3] Montana State University, Bozeman, MT

1. Abstract

Gearboxes and gears are part of the NASA Deep Space Network (DSN) antenna drives. The drives show backlash at the gearboxes and elevation bullgear due to a small gap between the gear teeth. Left uncorrected, backlash deteriorates the antenna pointing precision. Implementing two identical drives impose two non-identical torques. The torque difference (a.k.a. torque bias, or counter-torque) eliminates backlash. The electronic circuit at the axis drive generates the torque bias profile. The performance of the existing circuit is analyzed, and a modified circuit is designed that improves the antenna dynamics under external disturbances.

2. Introduction

Gearboxes and gears are components of the NASA Deep Space Network (DSN) antenna drives. A backlash phenomenon at the gearboxes and a bullgear is observed when one gear rotates through a small angle without causing a corresponding movement of the second gear. This eventually causes beating in the drives, gear wear, and deterioration of antenna tracking precision. In order to maintain antenna pointing precision the backlash phenomenon is eliminated by implementing two drives with a specific torque difference between them. The torque difference is called a torque bias, or counter-torque. With two motor configuration backlash clearance will occur at one drive while the other is still coupled. The antenna dynamics will be controlled by the latter drive. The effectiveness of the two-motor approach depends on the amount of torque bias applied at the drives, which depends on the antenna load. The torque bias should be large enough to lead the antenna through the gap for the maximal allowable torque load, but small enough that it will not cause excessive local stress, friction, or wear.

High and steady loads do not need a torque bias since the backlash is observed for low and reversing axis loads only. Time-varying loads, such as wind gusts, can produce high torques that become very low within a short period of time, causing a backlash gap when the torque bias dynamics are too slow. Reversing loads were observed at the DSS13 antenna site when wind gusting cause the drives to grind. Thus the proper dynamics of the torque bias-shaping loop were derived in this paper to assure antenna tracking precision.

3. Backlash and Its Prevention

Consider a simple gearbox with two gears rotating in opposite direction. Let the angle of rotation of the first gear be β_1, the second gear be β_2, the gearbox ratio be N, and the gearbox stiffness (at the second gear) be k. In this case the relationship between the gearbox rotation and the torque T at the second gear is as follows

$$T = \begin{cases} 0 & \text{for } |\Delta\beta| \le b \\ k(\Delta\beta - b) & \text{for } \Delta\beta > b \\ k(\Delta\beta + b) & \text{for } \Delta\beta < -b \end{cases} \qquad (1)$$

where $\Delta\beta = \beta_2 - \beta_1/N$, and b is the size of the backlash gap measured at the second gear. The plot of the torque versus the angle difference $\Delta\beta$ is shown in Fig.1 for $b=1$, and $k=20$. It is clear from the above equation that if the angle difference of two gears is smaller than the backlash gap b, there is a discontinuity in the gear motion, causing impacts of one gear tooth against the second gear tooth.

Implementing two driving gears instead of a single one will minimize the impact of this discontinuity. In this approach the driving torques T_1 and T_2 of the gears 1 and 2 are not identical but differ by the amount of ΔT. This difference is called the torque bias, or counter-torque. When both gears are driven and the backlash occurs at the first gear, the torque at the second driving gear is nonzero (it differs by ΔT), and the antenna is driven smoothly. This principle of "torque sharing" is used in the BWG antenna design.

The question remains how large the torque bias must be to prevent backlash. If the stiffness of the gearbox is k, the torque bias ΔT should be greater than $2kb$. But ΔT also depends on the load applied to the gears: No bias is required if torque load is high ($T_1 \cong T_2 >> \Delta T$) because the angle difference is large and the backlash is not observed even when $\Delta T = 0$. Plots of the existing profile of motor torque vs. axial load (as percentage of the maximal load) are shown in Fig.2, for 10, 20, and 30 percent of the bias. The bias is shaped such that it is the largest for the low loads, and phases-out to zero for higher loads.

In the event of dynamic loading, such as wind gusts, the optimal magnitude of the torque bias is not obvious. During dynamic loading, the torque difference determined for the steady-state case may not be large enough to prevent the backlash, and assuming a higher counter-torque may lead to premature wear. Additionally, quickly varying loads with small steady components may cause backlash in both gears simultaneously, despite the non-zero torque bias. Thus, the torque bias time response is also an important design factor.

The purpose of torque shaping analysis is to determine the value of the bias, the rate of phase-out, and the dynamics of the counter-torque circuit.

4. Friction

Friction is a torque that always opposes motion. The friction torque T_f depends of the relative velocity v of the moving surfaces. After motion begins friction is constant and referred to as the Coulomb friction torque T_c. At zero relative speed the friction torque T_f is equal and opposite to the applied torque T_o, unless the applied torque is larger than the stiction torque T_s. The latter is a torque at the moment of breakaway, and is larger than the Coulomb torque. A diagram of the friction torque versus relative velocity is shown in Fig.3. Denote $v_t > 0$, a velocity threshold, which is a small positive number then the friction torque is

$$T_f = \begin{cases} -T_c sign(v) & \text{for } |v| > v_t \\ -\min(|T_o|, T_s) sign(T_o) & \text{for } |v| \le v_t \end{cases} \qquad (2)$$

where T_o denotes the total applied torque, and *y=sign(x)* is a sign function: *y=1* for *x>0*, *y=-1* for *x<0*, and *y=0* for *x=0*. This equation states that if the surfaces in contact develop measurable relative velocity, such that $v > v_t$, the friction torque is constant and directed opposite to the relative speed. And if the relative velocity is small, within the threshold ($v \le v_t$) the friction torque does not exceed the stiction torque or the applied torque, and is directed opposite to the applied torque. The velocity threshold v_t is included for numerical purposes since the zero state does not exist, thus $v(i)$ is assumed zero if its absolute value is less than v_t.

In order to determine the friction torque T one must have the Coulomb friction torque T_c, the stiction (breakaway) torque T_s, the applied torque T_o, and the wheel rate v.

The Coulomb friction torque is proportional to the normal force at the surface F

$$T_c = \mu r F \qquad (3)$$

where r is the wheel radius, and μ is friction coefficient. For hard steel μ*=0.0012-0.002.*

The stiction (breakaway) torque T_s is the most often assumed to be slightly higher than the Coulomb friction

$$T_s = \alpha T_c, \qquad \alpha = 1.2 - 1.3 \tag{4}$$

The total applied torque, T_o, is determined as follows. Let the discrete state-space equation of the open-loop antenna be

$$x(i+1) = Ax(i) + B_u\, u(i) + B_f\, T(i), \tag{5a}$$

$$v(i) = Cx(i) \tag{5b}$$

where v is the antenna angular rate and T is the friction torque (either in azimuth or in elevation), and $(A,[B_u, B_f], C)$ is the state-space representation of the open-loop antenna. For the case of the antenna velocity within the threshold ($|v| \le v_t$) we assume $v=0$. Left-multiplying (5a) by C one obtains

$$v(i+1) = Cx(i+1) = CAx(i) + CB_u u(i) + CB_f T(i), \tag{6}$$

But $v(i+1) = 0$, thus

$$T(i) = -\frac{C}{CB_f}\left(Ax(i) + B_u u(i)\right), \tag{7}$$

and the applied torque, T_o, is opposite to the torque T, i.e.,

$$T_o(i) = \frac{C}{CB_f}\left(Ax(i) + B_u u(i)\right), \tag{8}$$

5. The Rate Loop Model with Friction and Backlash

The motions of the antenna in elevation and azimuth axes are uncoupled, therefore they are analyzed independently. The Simulink model of the elevation rate loop system is shown in Fig.4 (the following block diagrams are also Simulink diagrams). The model contains the antenna structure with an elevation rate input. The outputs are elevation encoder, elevation rate, elevation pinion rate, elevation and cross-elevation pointing errors. The antenna structure model is obtained from the DSS13 finite element model, as described in [1,2]. The elevation drive model which consists of the elevation rate input and elevation pinion rate inputs, and the elevation torque output is shown in Fig.5.

The drive consists of two motors (with gearboxes), denoted G_o, and the torque share circuit. Notation here is consistent with that of Refs.[1,2]. The block diagram of the subsystem G_o is shown in Fig.6. It consists of two amplifiers, a motor armature and a gearbox. The amplifiers and the motor armature are the same as those described in [1,2]. However, the gearbox model differs from the linear one, in that it includes the nonlinear friction and backlash models, see Fig.7. The friction torque in this model depends on the motor torque and the motor speed, as described earlier in Eq.(2). In the backlash model the torque depends on the difference between the motor and the pinion angle, as in Eq. (1). The torque share circuit, shown in Fig.5, is described later in this paper.

The accuracy of the rate-loop model was verified experimentally. Open-loop tests were conducted at the DSS26 antenna to compare the measured antenna dynamics with the simulated dynamics of the model that includes backlash and friction. The test data were used to determine the amount of friction, and the backlash angle. The rate-loop experiments were conducted by inserting the square-wave input of period 6.3 s and of amplitude 0.013 deg/s. Two tests were conducted: one with zero torque bias, and another with a torque bias of 15% of the maximal motor torque (the maximal torque is 308 kGm (26700 lb in), thus torque bias is 46 kGm (4000 lb in)).

For brevity of presentation we consider the elevation axis only. For zero torque bias the measured and simulated motor currents are shown in Fig.8a,b, and measured and simulated encoder reading in Fig.9a,b. These plots show satisfactory coincidence between the field data and simulation results. In particular, the measured motor currents, which are proportional to the motor torque, allowed us for the determination of the frictional torques.

The constant part of the current in Fig.8a is of 1 A. It corresponds to the constant rate of the antenna movement, since no inertia forces are present, and the motor effort is totally dedicated to overcome the friction forces. The 1 A current corresponds to the 61 kGm (5300 lb in) motor torque, or 9.1×10^5 kGm (7.9×10^7 lb in) axis torque, which is the amount of the friction torque.

For the 15% torque bias the plots of measured and simulated motor currents, and encoder readings are given in Figs. 10a,b, and 11a,b, respectively. This situation is different than the zero torque bias case in that the encoder show less chaotic movement of the antenna, and the motor torque plots indicate the presence of the torque bias, since their mean values are non-zero and have opposite sign.

6. Modifications of the Bias Profile

The torque share circuit is shown in Fig.12. Its purpose is to determine the torque bias that is appropriate for the antenna load. Thus the load in the form of motor current, *i*, is the circuit input. The fade-out voltage, f_o, is the additional voltage input that shapes the torque bias. The circuit output is the torque bias, v_b, (given in volts). The relationship between the current *i*, (which is the sum of currents i_1 and i_2), and the bias voltage v_b follows from the block-diagram, Fig.12

$$v_b = k_p \; sat(G_2 f_o + G_4|G_3 i|) \tag{9}$$

where G_2, G_3, and G_4 are the transfer functions 2, 3, 4, respectively, and k_p is the bias pot ($k_p = 0.8$). The parameters of the transfer functions are given in Table1.

The saturation function, *sat*, is defined as follows

$$sat(v) = \begin{cases} v_u & \text{if } v > v_u \\ v_l & \text{if } v < v_l \\ v & \text{elsewhere} \end{cases} \tag{10}$$

where the upper and lower limits of saturation are $v_u = 13\,\text{V}$, and $v_l = 0\,\text{V}$.

Table 1. Transfer function parameters

		old model	new model
filter 1	kctfr	4.54	66.67
	tau6	1.369	8.889
transfer function 1	ks	0.8	
	k1	716.197	
	tau1	6.37E-03	
transfer function 2	k2	-3.502	-2.114
	s2	1.093	0.8895
transfer function 3	k3	2	3.831
transfer function 4	k4	2.6*k2	1.617*k2

Note from the diagram in Fig.12 that the transfer functions G_2 and G_4 are proportional, that is

$$G_4 = k_2 G_2 \tag{11}$$

where $k_2 = 2.6$. Introducing (11) to (9) one obtains

$$v_b = k_p \; sat(G_2(f_o + k_2|G_3 i|)) \tag{12}$$

The steady state torque profile is obtained by replacing G_2 and G_3 with the corresponding DC gains, which are

$$G_3(0) = -1, \tag{13a}$$

and

$$g_2 = G_2(0) = -3.20 \tag{13b}$$

Thus, for the steady state, the bias voltage equation (12) becomes the following

$$v_b = k_p \; sat(g_2(f_o + k_2|i|)) \tag{14}$$

The plot of v_b versus i (proportional to the axis torque), for $k_p = 0.7$, $g_2 = -3.20$, $f_o = -9\,\text{V}$, and $k_2 = 2.6$ (as implemented at DSS13) is shown in Fig.13a as a solid line.

The bias can be shaped in three ways:

- By extending the constant value of the bias,
- By changing the constant value of the bias
- By changing the slope of the bias

From (14) it follows that the first modification (the extension of the constant value of the bias) is obtained by changing the value of the fade-out voltage f_o. The bias profile for the three different fade-out voltages is shown in Fig.13a: dashed line for the fade-out voltage of -7 V, solid line for the fade-out voltage of -9 V, and dashed-dot line for the fade-out voltage of -11 V. The higher (in absolute value) voltage, the wider is the constant value of the bias.

By inspection of Eq.(14) one finds that the second modification (varying the constant value of torque bias) is obtained by varying the bias pot, k_p. The plots of bias voltage vs. counter-torque current for bias pots of 0.3 (dashed-dot line), 0.5 (dashed line), and 0.7 (solid line) are shown in Fig.13b. The plot shows that larger bias pot result in larger bias voltages.

The slope is changed by the varying the gain g_2 of transfer function TF2. This is illustrated in Fig.13c with three cases of gain scaling: the nominal gain, $g_2 = -3.20$ (solid line), the two-fold increased gain, $g_2 = -6.40$ (dashed line), and the reduced gain, $g_2 = -2.24$ (dashed-dotted line). The plots show that smaller gains result in smaller slopes.

Finally, from Eq.(14) it follows that bias voltage depends on the gain k_2. This relationship is shown in Fig.13d, where the slope and horizontal extension of the bias are varied simultaneously after modifying k_2.

To prevent backlash in extreme dynamic loads a flatter bias voltage is preferred, so gains g_2 and k_2 were modified according to the above relationships. The dashed line in Fig.14 shows the bias voltage profile for $g_2 = -2.38$ and $k_2 = 1.617$. This slope is smaller, as compared with the nominal, solid line. The resulting profile (as percentage of the maximal torque) is shown in Fig.15, for 10, 20, and 30 percent of the bias. Compare this profile with that of the existing torque bias (Fig.3) and note the sharp decline for the existing configuration compared to the mild slopes of the modified design.

The performance of the old and new models has been verified analytically and in field testing the rate-loop model. The bias voltage is chosen as a indicator of the quality of design. For best design results the bias should remain at the maximum value; in an acceptable design the bias would always be non-zero; if the bias remains at even for small the backlash is observed and the design has not achieved it's goals. The differences between these two designs can be exposed during high loads that vary abruptly. Therefore a saw-tooth wave has been chosen as a test signal to be applied at the antenna rate loop input, with amplitude of 0.685 deg/s (85% of the maximal rate), and period 5 sec, see Fig.16. The bias voltage of the old design with a saw-tooth input is shown in Fig.17, solid line (measured at DSS26 antenna), and in Fig.17, dashed line (simulated using an analytical model). Both plots show a bias voltage that varies extensively, and remains at zero for significant periods. The maximal bias is 11.2 V (field data) and 10.4 (analysis), which are 86% and 80% of the maximal bias, respectively. The test results for the new design are shown in Fig.18, solid line (field data), and Fig.18, dashed line (simulations). Both show non-zero bias that varies from 8.0 to 11.4V (field data) and from 7.2 to 11.6V (analysis). This translates to 62-87% of maximal bias (field data) and into 56-88% of maximal bias (analysis). Data shows that the bias torque performance has significantly improved.

7. Improvements of the Bias Torque Dynamics

The filter marked Filter 1 in the drive block diagram Fig.6 is responsible for the torque bias dynamics. Its transfer function is as follows

$$G_1 = \frac{k_{ctfr}}{1+\tau_6 s} \tag{15}$$

with gain $k_{ctfr} = 3.31$, and time constant $\tau_6 = 0.73\ s$. These filter constants are taken from the current design.

Denote i_1 and i_2 the currents of motor 1 and motor 2. The torque bias is proportional to their difference $\Delta i = i_2 - i_1$. A simulated experiment in which a zero rate command was applied recorded the relative torque bias $(\Delta i / i_{\max}) * 100\%$. The initial torque bias was set to 0, and in the first period of antenna response that torque bias raised to its nominal value (22%). The response is illustrated in Fig.19a with the (nominal) time constant of $\tau_6 = 0.73\ s$ and variable gains k_{ctfr} of 3.31. The figure shows that overshoot is significant, and that settling time is over 2 s.

After examining the impact of Filter 1 time constant and gain on counter-torque dynamics, $\tau_6 = 0.1125\ s$ and $k_{ctfr} = 48.67$ were chosen for the new time constant and gain. Counter-torque dynamics resulting from the above parameters are shown in Fig.19b, where overshoot (0%) and settling time (0.8 s) have improved significantly.

8. Conclusions

In this project the 34m DSN antenna backlash and friction were measured, modeled, and simulated. The torque-shaping circuit was analyzed, and a new bias torque profile was developed. The new profile has flatter slopes, allowing for milder torque bias variations regardless of load. The torque bias dynamics are shaped with Filter 1 of the drive system. The existing filter parameters cause large torque bias overshoot (80%), and settling time (2.4 s). The new filter causes no overshoot, and a settling time of just 0.8 s. This torque-

shaping circuit and filter were tested in the field confirming the improved antenna performance.

Acknowledgement

The research described in this paper was carried out at the Jet Propulsion Laboratory, California Institute of Technology, under a contract with the National Aeronautics and Space Administration.

9. References

1. W. Gawronski and J.A.Mellstrom, "Modeling and Simulations of the DSS 13 Antenna Control System," *TDA Progress Report, 42-105*, 1991.
2. Gawronski, W., and J.A. Mellstrom, "Control and Dynamics of the Deep Space Network Antennas," a chapter in *Control and Dynamic Systems*, vol.63, ed. C.T. Leondes, Academic Press, San Diego, 1994.

FIGURE CAPTIONS:

Figure 1. The backlash function

Figure 2. Motor torque vs. axial torque, for 10% (dashed line), 20% (solid line), and 30% (dot-dashed line) torque bias.

Figure 3. Friction torque vs. relative velocity

Figure 4. Elevation rate-loop system

Figure 5. Elevation drive

Figure 6. Motor, gearbox, and amplifier (system G_o)

Figure 7. Motor mechanical properties and gearbox

Figure 8. Motor currents for zero torque bias: (a) measured and (b) simulated.

Figure 9. Encoder readings for zero torque bias: (a) measured and (b) simulated.

Figure 10. Motor currents for 15% torque bias: (a) measured and (b) simulated.

Figure 11. Encoder readings for 15% torque bias: (a) measured and (b) simulated.

Figure 12. The torque share circuit.

Figure 13. Bias voltage vs. axis torque: a) for the three different fade-out voltages: -7 V (dashed line), -9 V (solid line), and -11 V (dashed-dot line), b) for the bias pots of 0.3 (dashed-dot line), 0.5 (dashed line), and 0.7 (solid line), c) for three cases of DC gain: nominal gain, $g_2 = -3.20$ (solid line), two-fold increased gain, $g_2 = -6.40$ (dashed line), and the reduced gain, $g_2 = -2.24$ (dashed-dotted line), d) for the gain $k_2 = 2.1$ (dashed line), $k_2 = 2.6$ (solid line), and $k_2 = 3.1$ (dash-dotted line).

Figure 14. Bias voltage vs. axis torque for $g_2 = -2.38$ and $k_2 = 1.617$ (dashed line), and for the existing gains (solid line).

Figure 15. Modified profile of motor torque vs. axial torque, for 10% (dashed line), 20% (dot-dashed line), and 30% (solid line) torque bias.

Figure 16. Test signal

Figure 17. Bias voltage under test signal for the old circuit design: from field tests (solid line), and from analysis (dashed line).

Figure 18. Bias voltage under test signal for the new circuit design: from field tests (solid line) and from analysis (dashed line).

Figure 19. Counter-torque dynamics a) for $\tau_6 = 0.73\,\text{s}$, $k_{ctfr} = 3.31$, and for $\tau_6 = 0.1125\,\text{s}$, $k_{ctfr} = 48.67$.

Figure 1

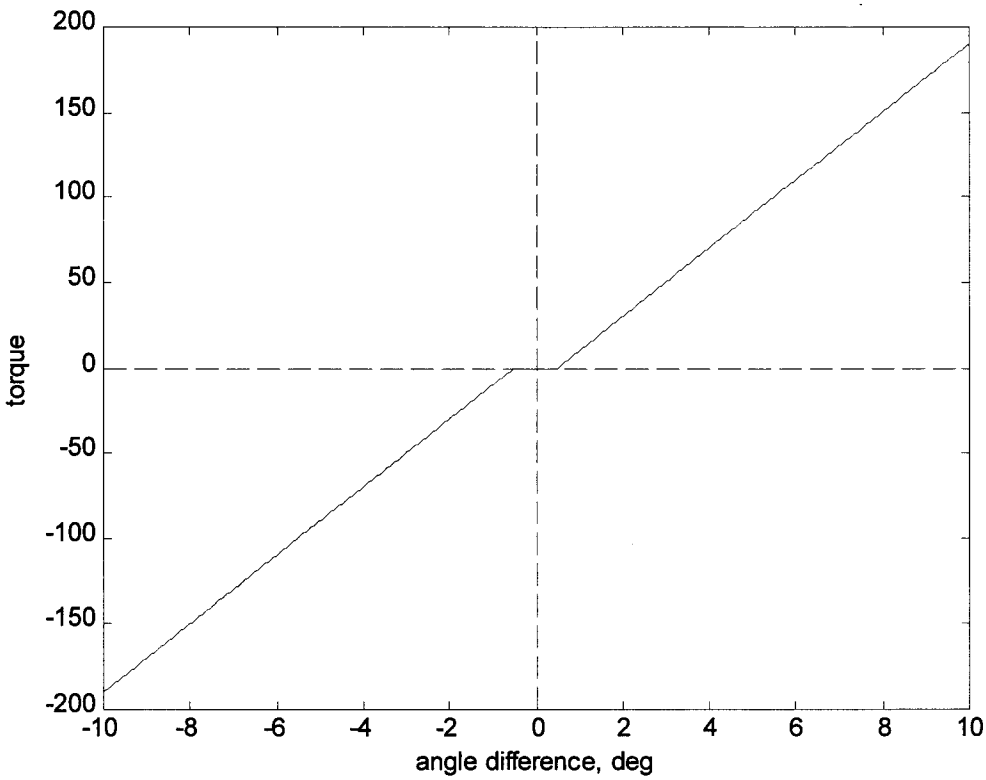
200
150
100
50
0
-50
-100
-150
-200
torque
-10
-8
-6
-4
-2
0
2
4
6
8
10
angle difference, deg

Figure 2

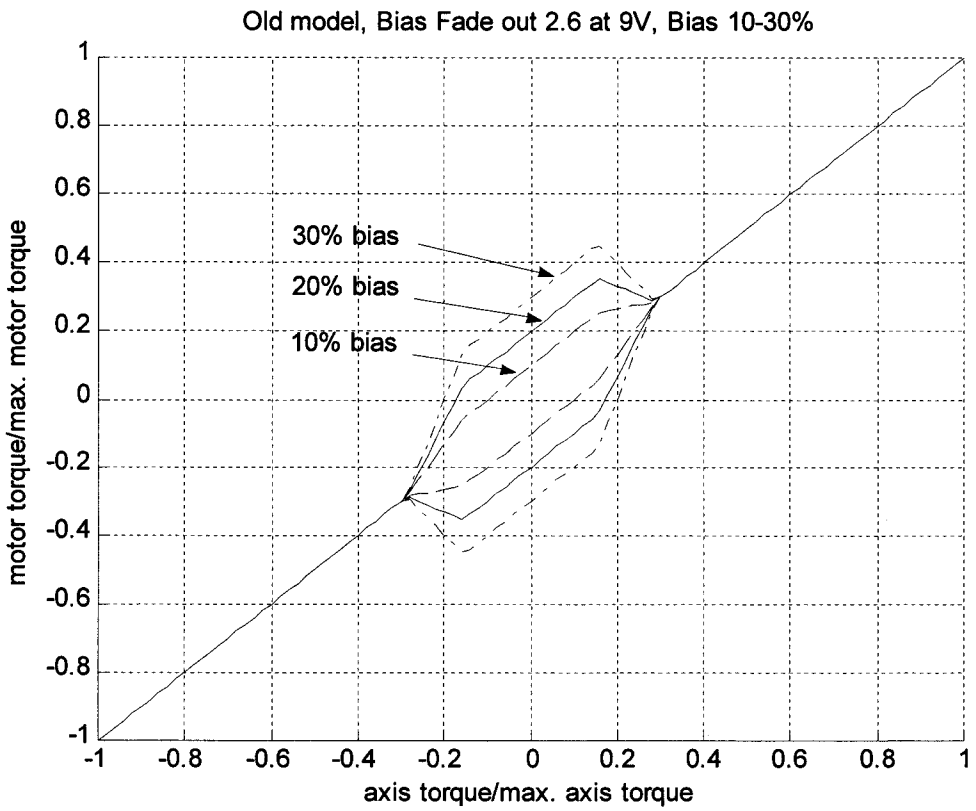
Old model, Bias Fade out 2.6 at 9V, Bias 10-30%
30% bias
20% bias
10% bias
motor torque/max. motor torque
axis torque/max. axis torque
1
0.8
0.6
0.4
0.2
0
-0.2
-0.4
-0.6
-0.8
-1
-1
-0.8
-0.6
-0.4
-0.2
0
0.2
0.4
0.6
0.8
1

Figure 3

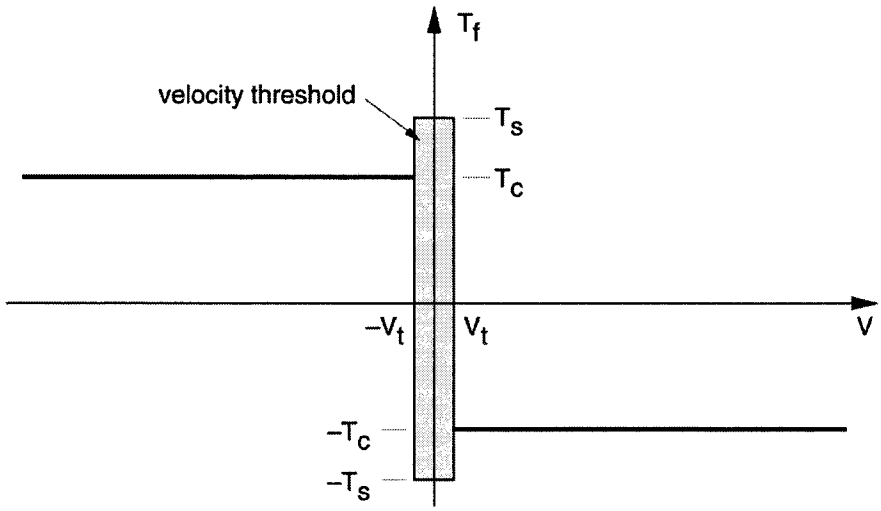

Figure 4

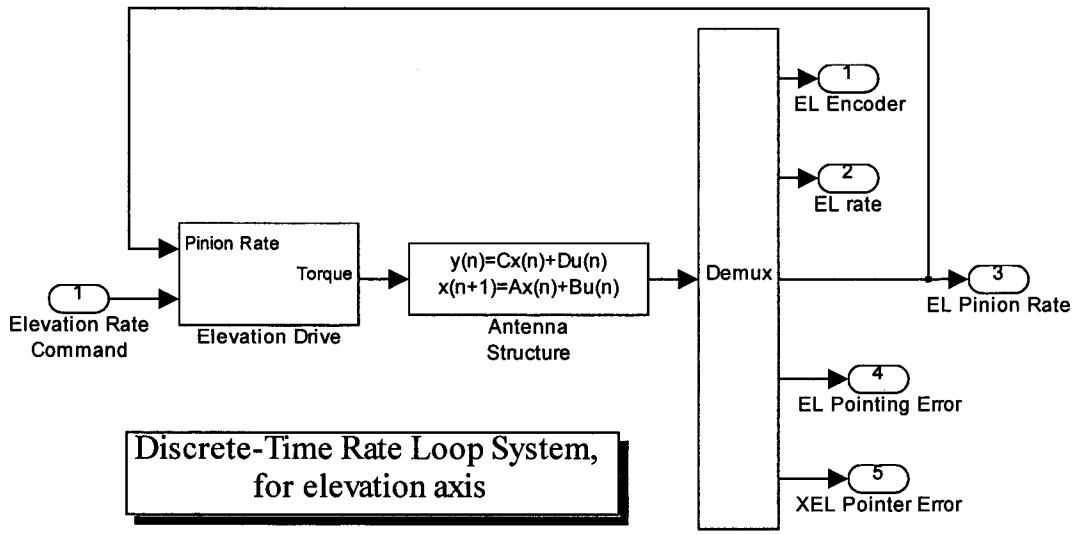

Discrete-Time Rate Loop System, for elevation axis

Figure 5

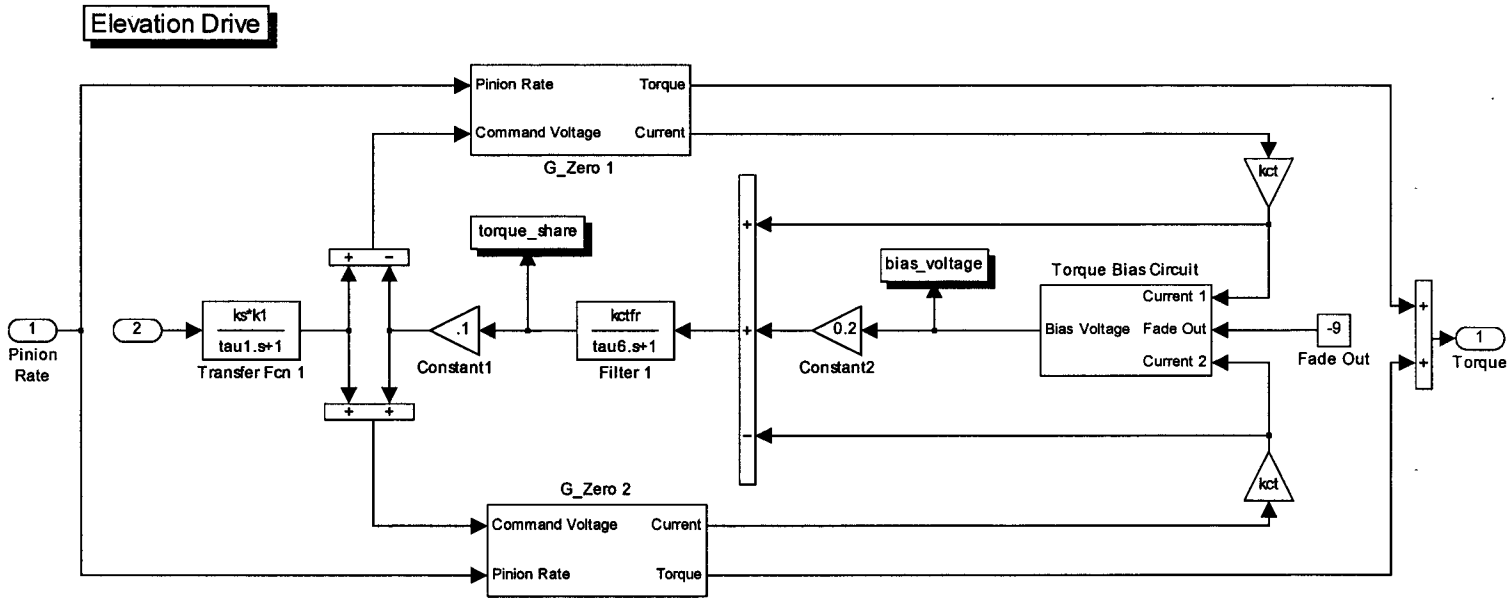
Elevation Drive
Pinion Rate
Torque
Command Voltage
Current
G_Zero 1
kct
torque_share
bias_voltage
Torque Bias Circuit
Current 1
Bias Voltage
Fade Out
Current 2
-9
Fade Out
1
Pinion Rate
2
ks*k1
tau1.s+1
Transfer Fcn 1
.1
Constant1
kctfr
tau6.s+1
Filter 1
0.2
Constant2
1
Torque
G_Zero 2
Command Voltage
Current
Pinion Rate
Torque

Figure 6

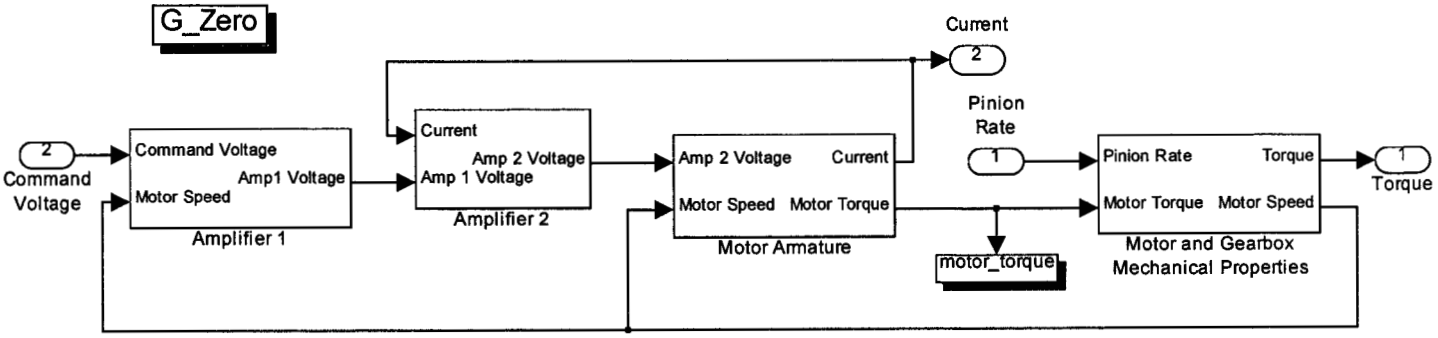
G_Zero
Current
2
Pinion
Rate
1
2
Command
Voltage
Command Voltage
Motor Speed
Amp1 Voltage
Amplifier 1
Current
Amp 2 Voltage
Amp 1 Voltage
Amplifier 2
Amp 2 Voltage
Current
Motor Speed
Motor Torque
Motor Armature
motor_torque
Pinion Rate
Torque
Motor Torque
Motor Speed
Motor and Gearbox
Mechanical Properties
1
Torque

Figure 7

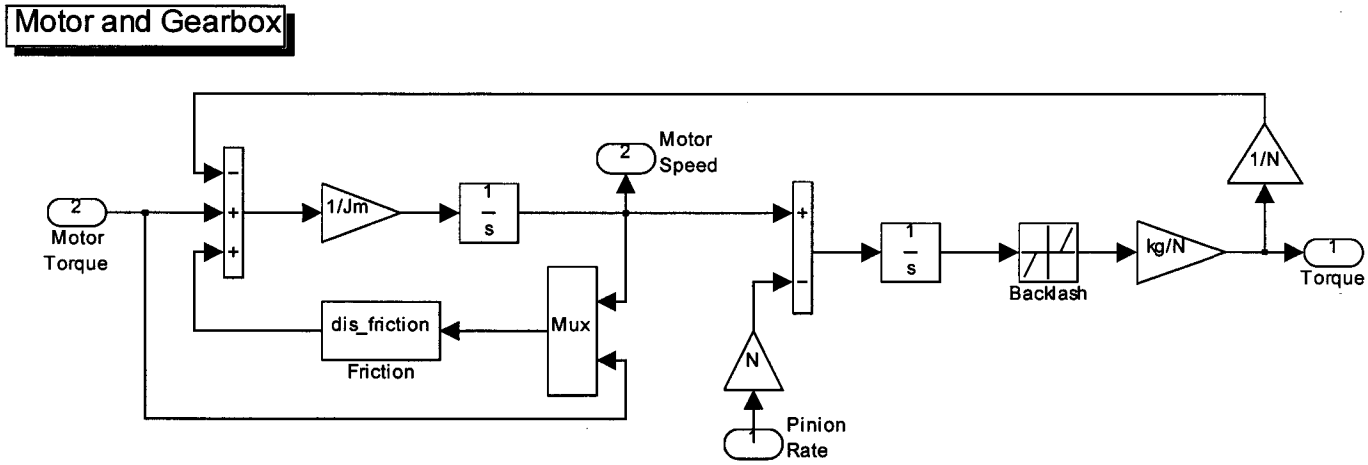
Motor and Gearbox
2
Motor
Torque
1/Jm
1
s
2
Motor
Speed
dis_friction
Friction
Mux
N
1
Pinion
Rate
1
s
Backlash
kg/N
1/N
1
Torque

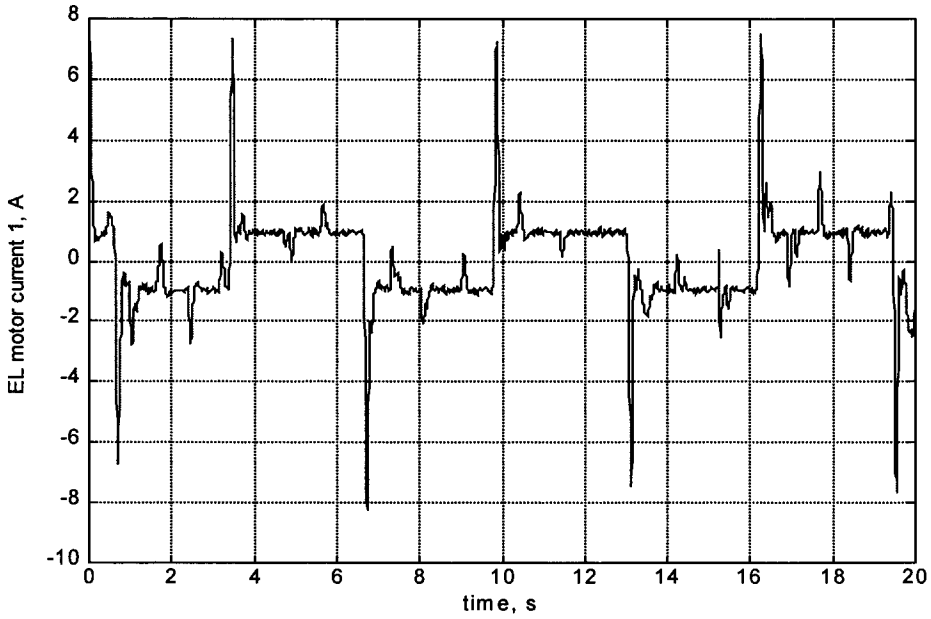
EL motor current 1, A
time, s
8
6
4
2
0
-2
-4
-6
-8
-10
0
2
4
6
8
10
12
14
16
18
20

Figure 8 a,b

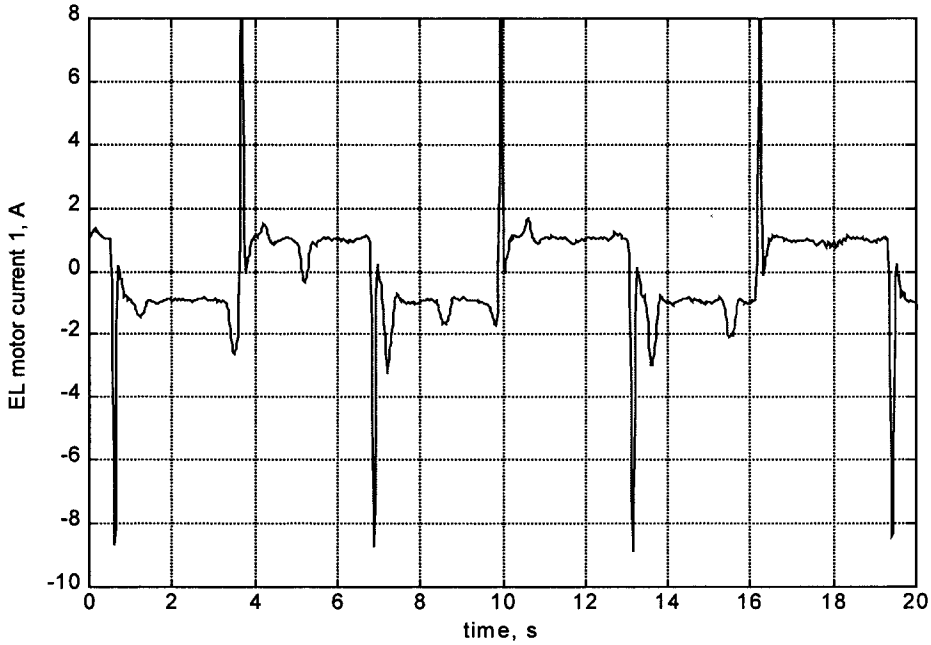
EL motor current 1, A
time, s
8
6
4
2
0
-2
-4
-6
-8
-10
0
2
4
6
8
10
12
14
16
18
20

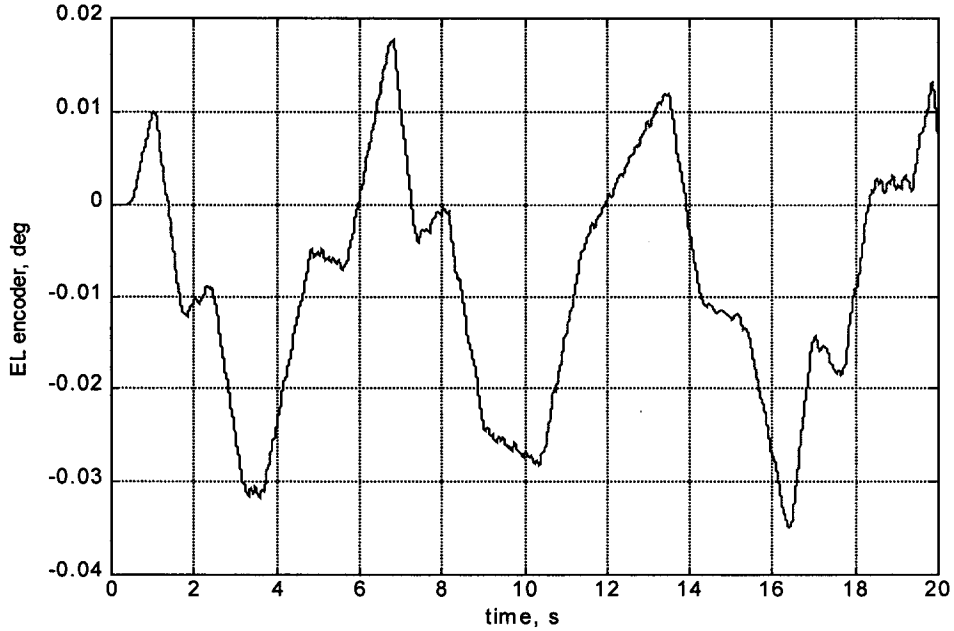
0.02
0.01
0
-0.01
-0.02
-0.03
-0.04
EL encoder, deg
0
2
4
6
8
10
12
14
16
18
20
time, s

Figure 9 a,b

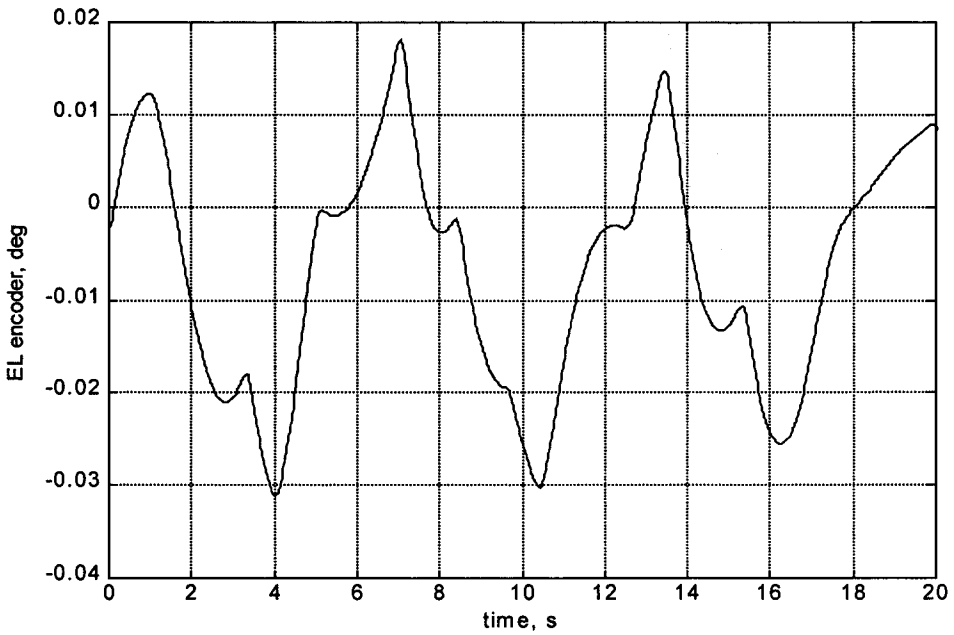
0.02
0.01
0
-0.01
-0.02
-0.03
-0.04
EL encoder, deg
0
2
4
6
8
10
12
14
16
18
20
time, s

Figure 10 a,b

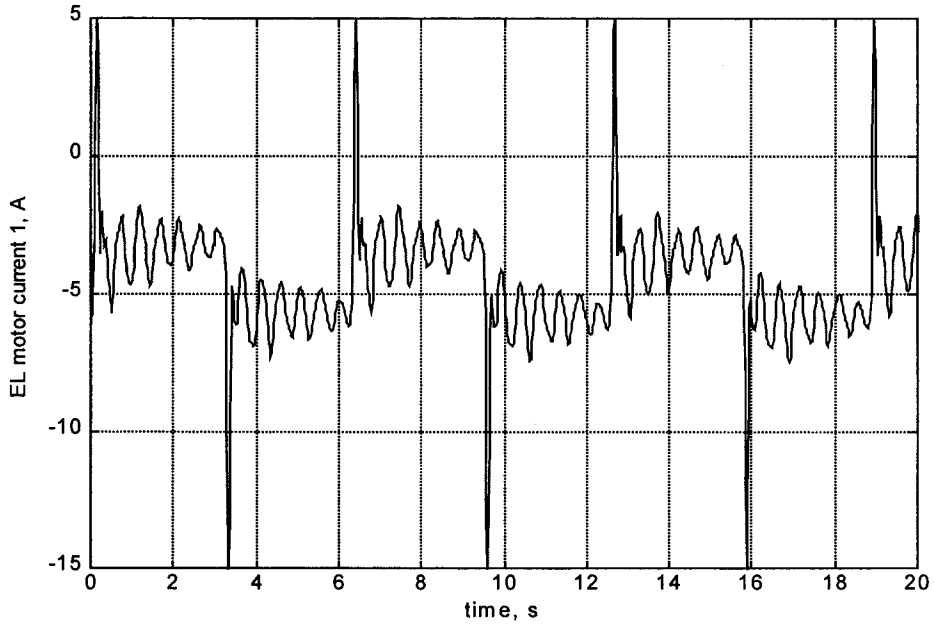
5
0
-5
-10
-15
EL motor current 1, A
0
2
4
6
8
10
12
14
16
18
20
time, s

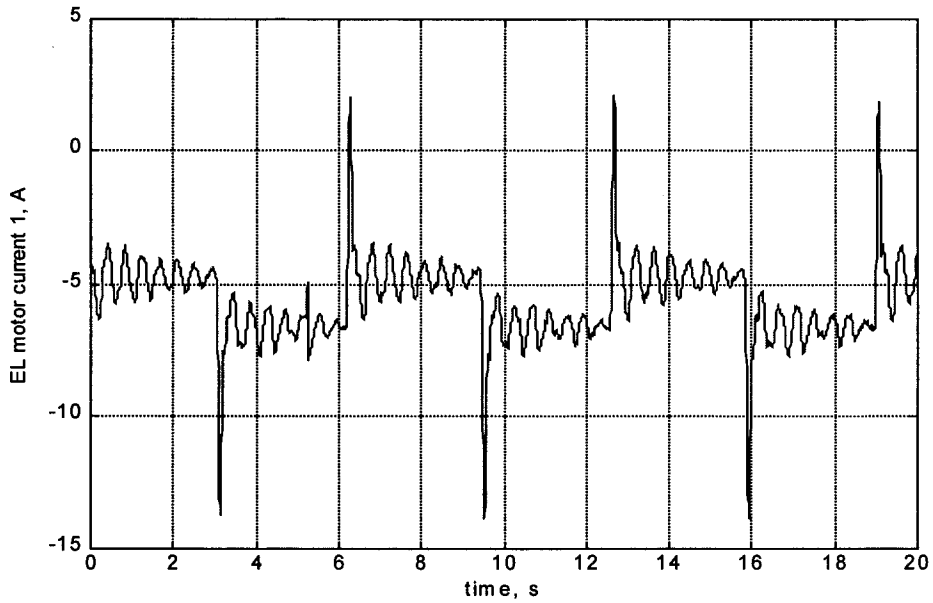
5
0
-5
-10
-15
EL motor current 1, A
0
2
4
6
8
10
12
14
16
18
20
time, s

Figure 11 a,b

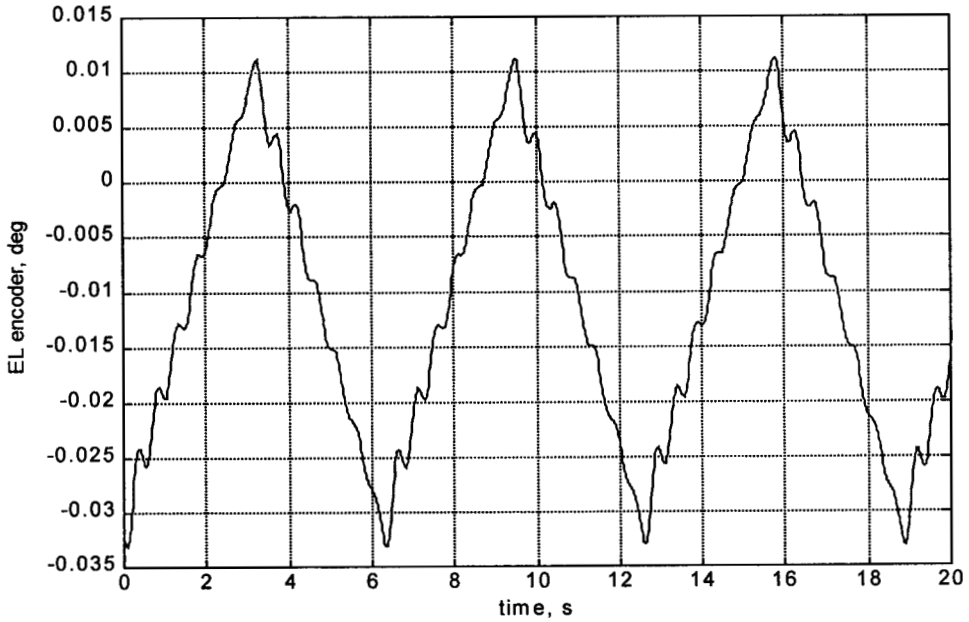
0.015
0.01
0.005
0
-0.005
-0.01
-0.015
-0.02
-0.025
-0.03
-0.035
EL encoder, deg
0
2
4
6
8
10
12
14
16
18
20
time, s

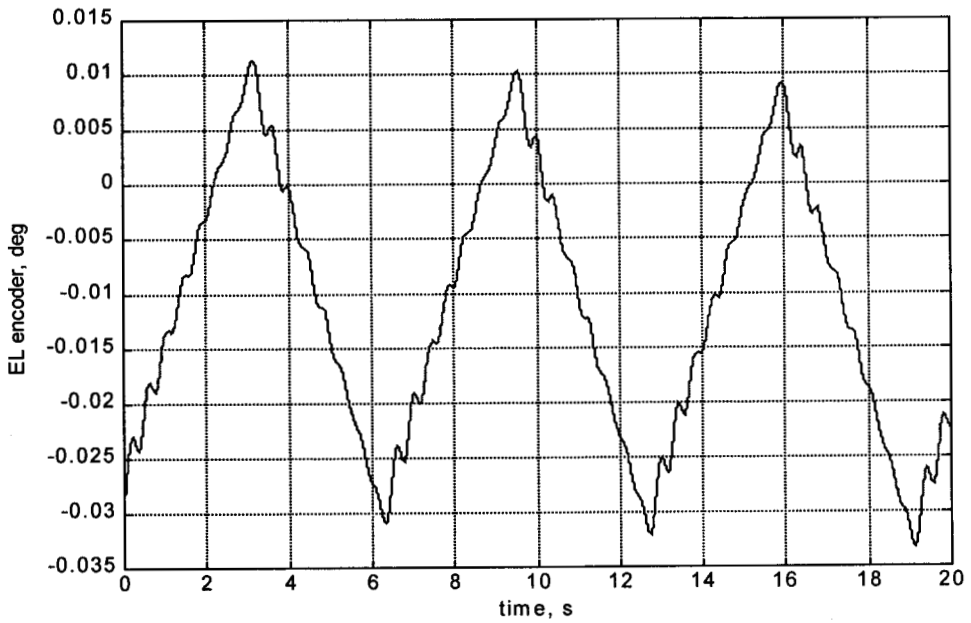
0.015
0.01
0.005
0
-0.005
-0.01
-0.015
-0.02
-0.025
-0.03
-0.035
EL encoder, deg
0
2
4
6
8
10
12
14
16
18
20
time, s

Figure 12

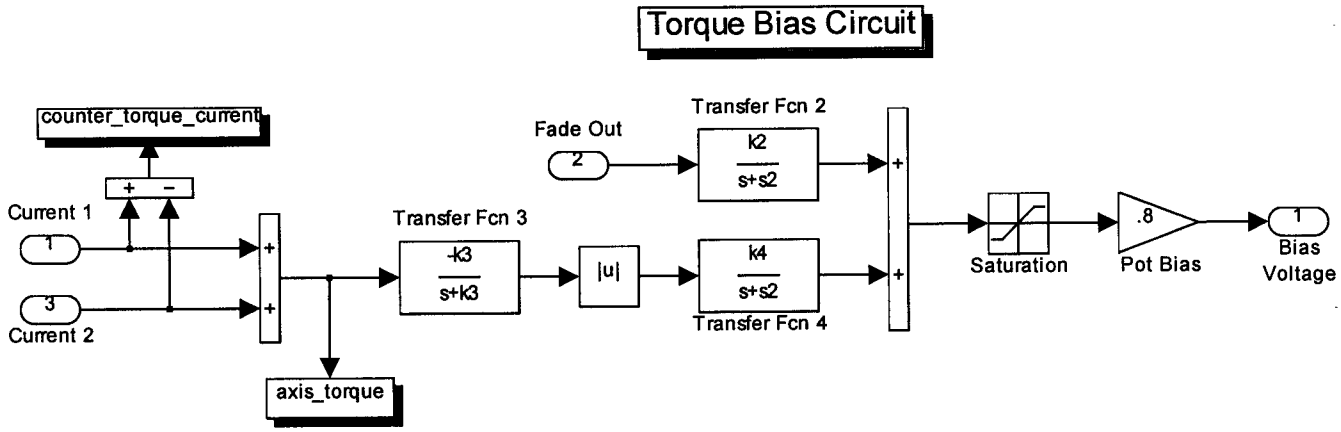
Torque Bias Circuit
counter_torque_current
Current 1
1
3
Current 2
+
-
+
+
axis_torque
Transfer Fcn 3
-k3
s+k3
|u|
Fade Out
2
Transfer Fcn 2
k2
s+s2
k4
s+s2
Transfer Fcn 4
+
+
Saturation
.8
Pot Bias
1
Bias
Voltage

Figure 13

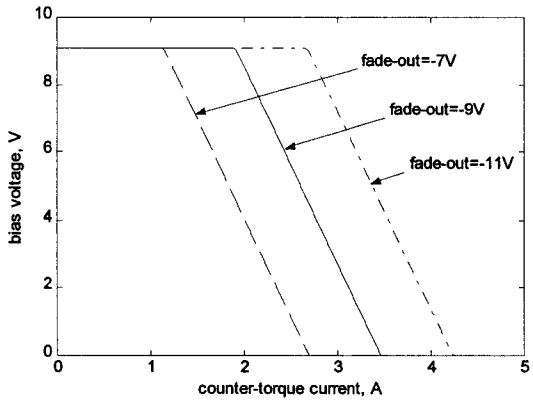
fade-out=-7V
fade-out=-9V
fade-out=-11V
bias voltage, V
counter-torque current, A

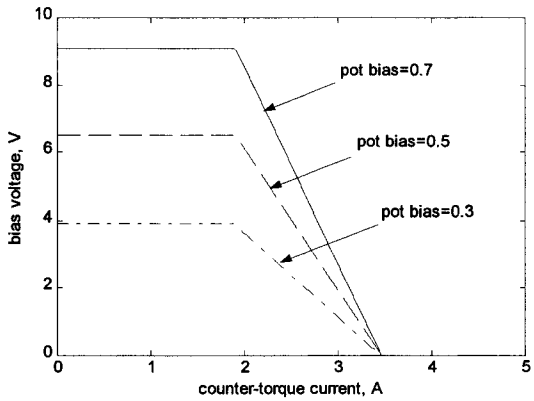
pot bias=0.7
pot bias=0.5
pot bias=0.3
bias voltage, V
counter-torque current, A

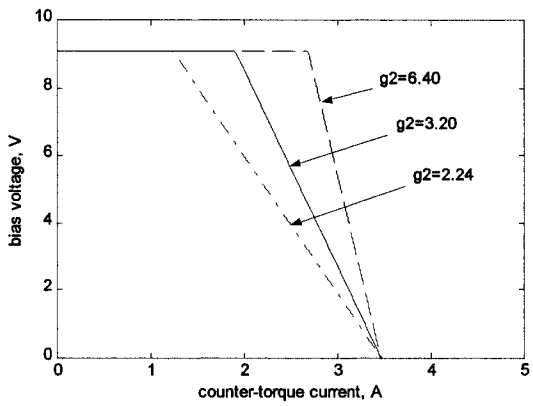
g2=6.40
g2=3.20
g2=2.24
bias voltage, V
counter-torque current, A

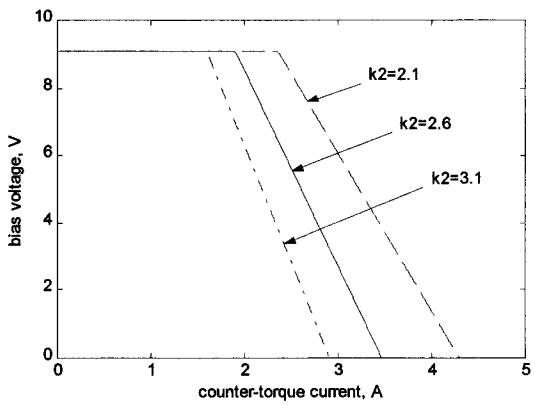
k2=2.1
k2=2.6
k2=3.1
bias voltage, V
counter-torque current, A

Figure 14

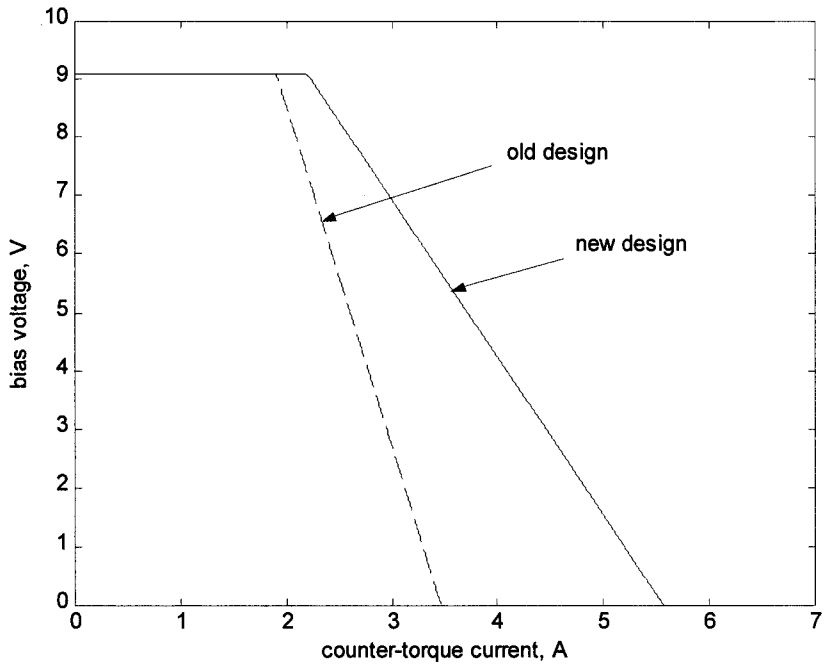
10
9
8
7
6
5
4
3
2
1
0
bias voltage, V
0
1
2
3
4
5
6
7
counter-torque current, A
old design
new design

Figure 15

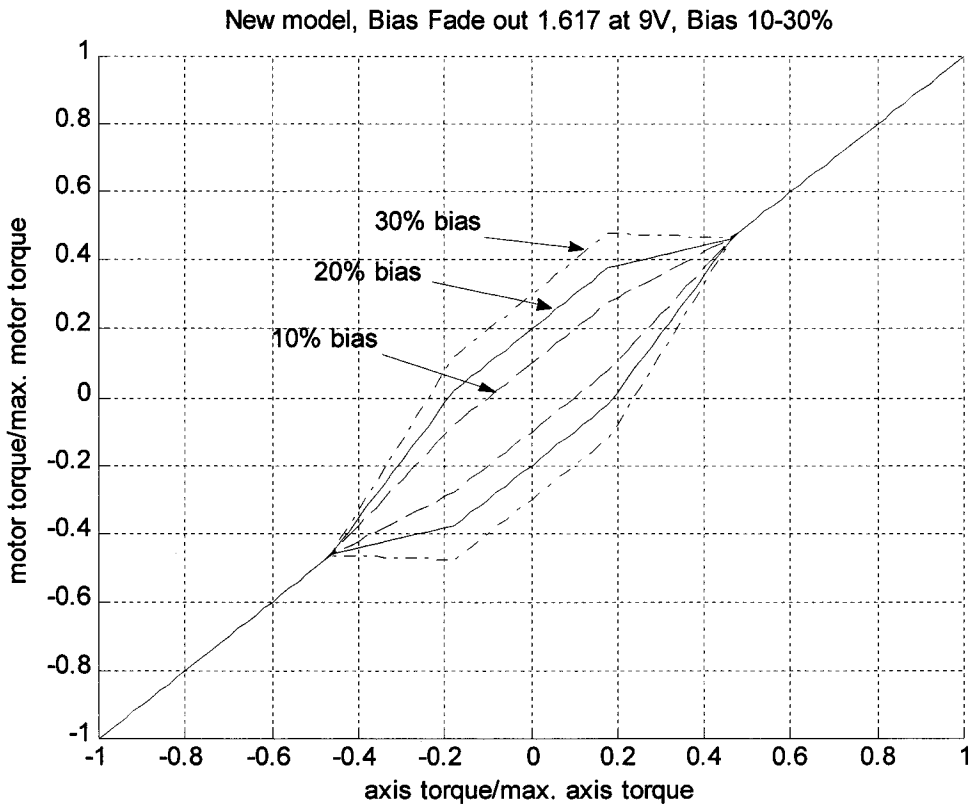
New model, Bias Fade out 1.617 at 9V, Bias 10-30%
30% bias
20% bias
10% bias
motor torque/max. motor torque
axis torque/max. axis torque
1
0.8
0.6
0.4
0.2
0
-0.2
-0.4
-0.6
-0.8
-1
-1
-0.8
-0.6
-0.4
-0.2
0
0.2
0.4
0.6
0.8
1

Figure 16

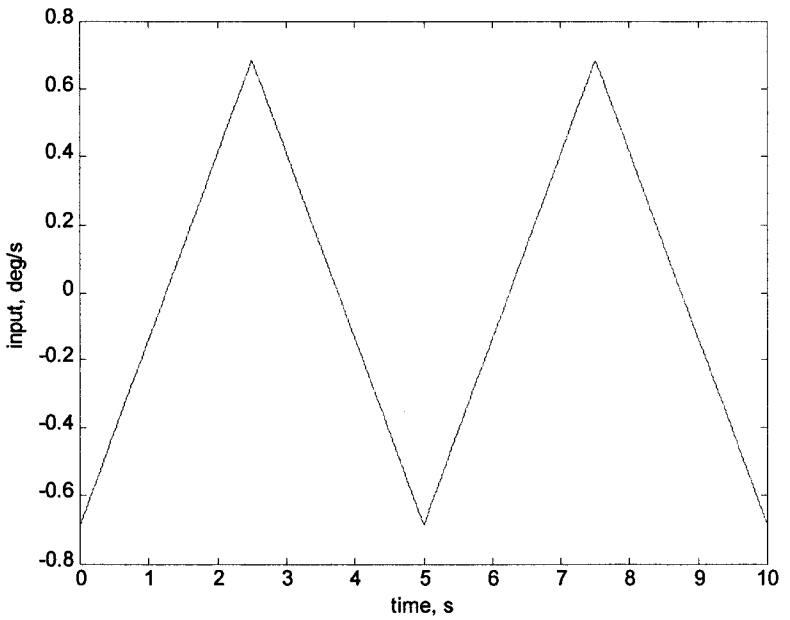

Figure 17

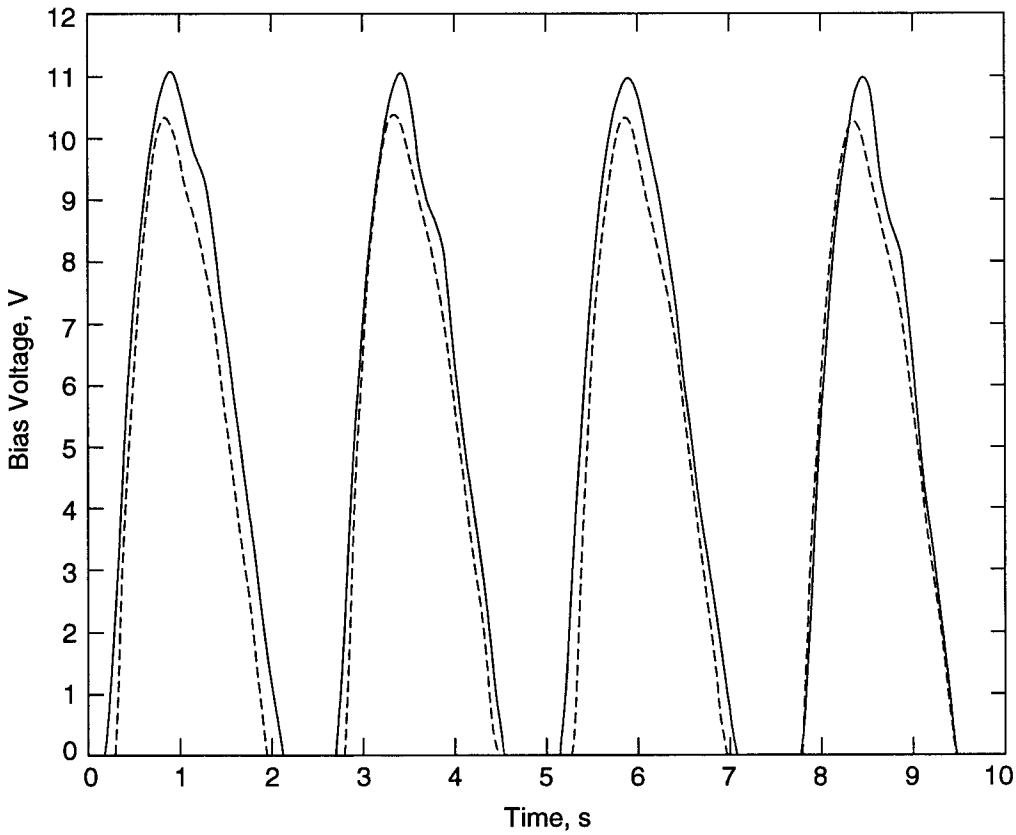

Figure 18

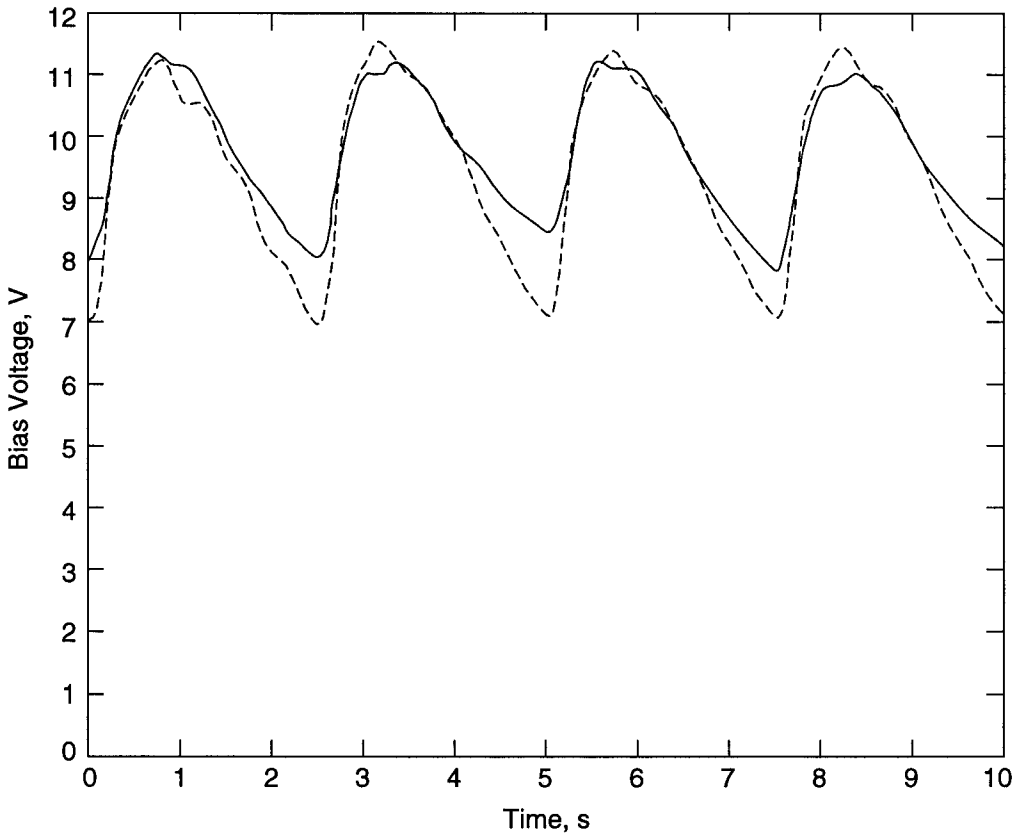

Figure 19

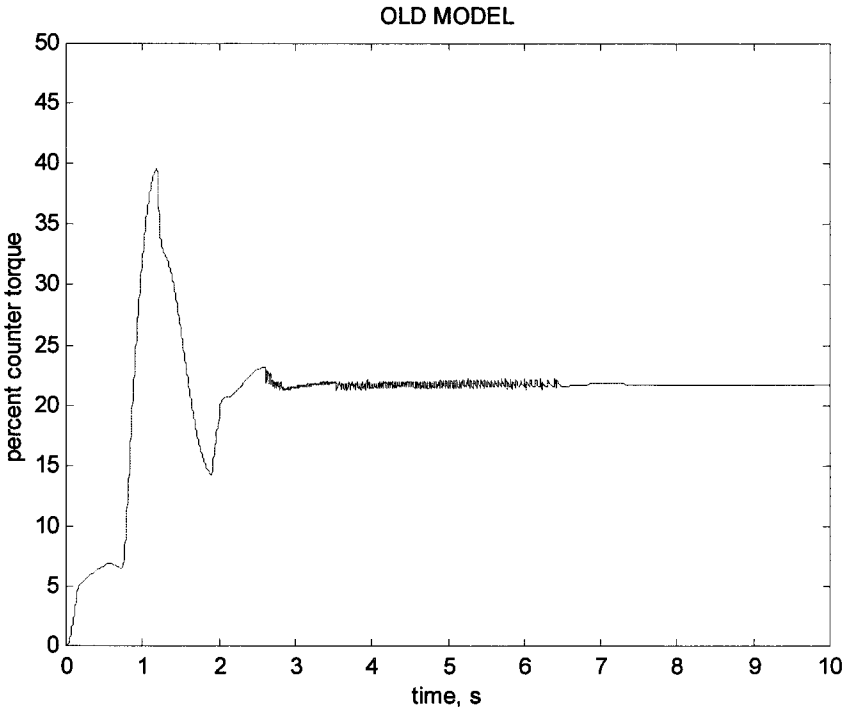
OLD MODEL
percent counter torque
time, s
0
5
10
15
20
25
30
35
40
45
50
0
1
2
3
4
5
6
7
8
9
10

a)

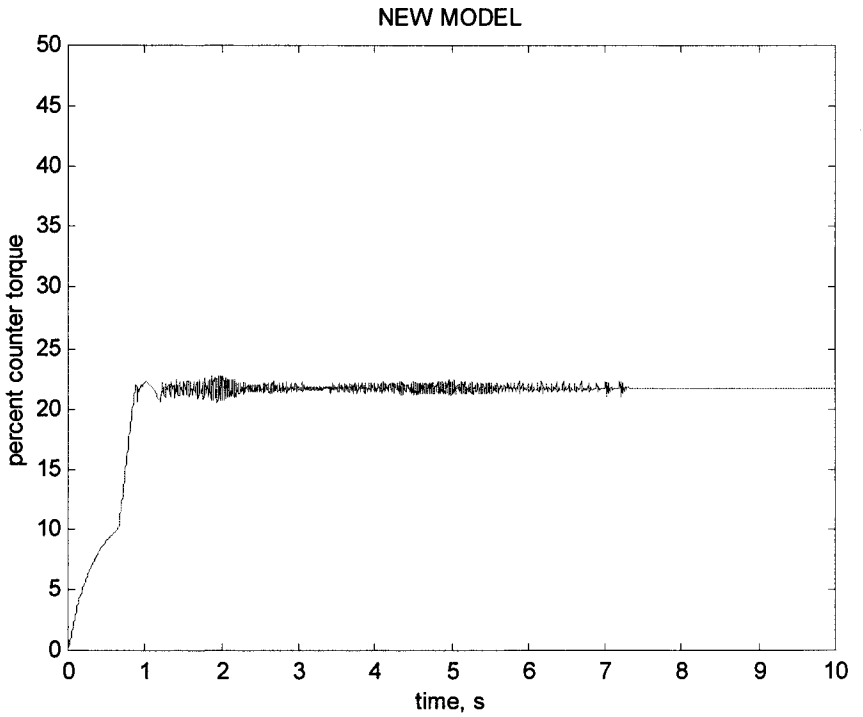
NEW MODEL
percent counter torque
time, s
0
5
10
15
20
25
30
35
40
45
50
0
1
2
3
4
5
6
7
8
9
10

b)